ISSN 1997-1400 Int. J. Pavement Res. Technol. 5(3):142-152

A Laboratory Investigation into the Effect of Long-Term Oven Aging on RAP Mixes Using Dynamic Modulus Test

Dharamveer Singh[1+], Musharraf Zaman[2], and Sesh Commuri[3]

Abstract: Reclaimed Asphalt Pavement (RAP) has been widely used in the construction and rehabilitation of flexible pavements. A proper understanding of the performance of hot mix asphalt (HMA) prepared with RAP is important to ensure better and longer lasting pavements. The present study was undertaken to evaluate the effect of long-term oven (LTO) aging of HMA mixes containing RAP using the dynamic modulus (|*E**|) test. Two different HMA mixes, namely Mix-1 and Mix-2, were collected from asphalt plant. Mix-1 contains performance grade (PG) 64-22 unmodified binder mixed with 25% RAP, while Mix-2 includes PG76-28 styrene-butadiene-styrene (SBS)-modified binder mixed with 15% RAP. Both mixes have the same aggregate type (primarily limestone), aggregate gradation and binder content. Specimens were compacted using a Superpave Gyratory Compactor (SGC) at four target air voids of 6%, 8%, 10% and 12% (i.e., percentage compactions of 94% to 88% of the maximum theoretical density). LTO-aging of compacted specimens was done in accordance with AASHTO R30. |*E**| tests were conducted on un-aged and LTO-aged compacted specimens at four different temperatures of 4^{o}C, 21^{o}C, 40^{o}C and 55^{o}C and at six different loading frequencies of 25 Hz, 10 Hz, 5 Hz, 1 Hz, 0.5 Hz and 0.1 Hz. Mix-1, with a softer grade binder (i.e., PG64-22) and a higher amount of RAP (25%), had a higher |*E**| compared to Mix-2 with a stiffer grade binder (i.e., PG76-28) and lesser amount of RAP (15%). Furthermore, statistical analyses using the standard "student t-test" revealed that, irrespective of binder grade, higher amounts of RAP result in stiffer mixes with higher |*E**|. LTO-aging increased |*E**| of the compacted samples by 42% to 60%, depending on the amount of RAP and air void content in the compacted specimen. It is expected that the present study will be helpful in understanding the behavior of HMA mixes containing RAP.

Key words*: Dynamic modulus; Hot mix asphalt; Reclaimed asphalt pavement.*

Introduction

Reclaimed asphalt pavement (RAP) is a recycled pavement material containing coated aggregates with asphalt binder [1-3]. According to the U.S. Environmental Protection Agency and the Federal Highway Administration, about 90 million tons of asphalt concrete is reclaimed each year, and over 80 percent (73 million tons) of it is reused in the production of hot mix asphalt (HMA) [3]. The use of RAP in a HMA mix has been favored over the use of virgin materials because it saves cost of raw materials and reduces the environmental impact of discarded pavement materials [1, 3-5]. Furthermore, the addition of RAP is beneficial in resisting permanent deformation at higher temperature [6-12]. On the other hand, excessive RAP content may reduce the resistance to cracking at low temperatures [13].

Many studies have been done to evaluate the effect of RAP on the performance of asphalt mix. McDaniel et al. [14] reported that adding small amounts of RAP does not significantly alter mix properties. As RAP content increases, some effects on mix properties were noted. However, the change was not in proportion to the amount of added RAP. Similarly, Kandhal et al. [15] found that up to 15% RAP can be used without changing the PG binder grade. In general, most studies on laboratory-produced mixes conclude that the effect of RAP on mixes' properties is negligible at RAP contents within 15% to 20% [13-14, 16-17]. A low RAP content does not significantly affect the stiffness and strength of a mix at low and high temperatures. However, an increase in RAP content beyond 20% increases the mix's stiffness and strength, resulting in an increase in its rutting resistance [2, 7, 13-14, 18].

Limited studies have been conducted thus far to investigate the effect of long-term oven (LTO)-aging on plant produced HMA mixes prepared with RAP. Daniel et al. [19] and Francken et al. [20] studied the effect of aging on HMA mixes. Specimens were compacted and subjected to three different levels of long-term aging. It was reported that LTO-aging increases dynamic modulus (|*E**|) of the compacted samples significantly. However, they did not study the effect of aging on mix containing RAP. Evaluation of the effect of short-term and long-term aging on the performance of RAP-containing mixes would be helpful in understanding the response (stress-strain behavior) of a flexible pavement.

Furthermore, it is known that for a given virgin HMA mix (without any RAP), a mix with stiffer binder grade (i.e., PG 76-28) is expected to result in a higher |*E**| compared to a mix with a softer binder grade (i.e., PG 64-22). However, such behavior may not be reflected in a mix containing RAP, because it changes the rheological property and grade of the binder (compared to the virgin mix). Hence, it becomes important to evaluate the performance of RAP-containing HMA mixes at the design phase of a flexible pavement.

[1] School of Civil Engineering and Environmental Science, University of Oklahoma, 202 W. Boyd Street, Norman, Oklahoma, USA, 73019.
[2] College of Engineering, University of Oklahoma, Norman, Oklahoma, USA, 73019.
[3] School of Electrical and Computer Engineering, University of Oklahoma, Norman, Oklahoma, USA, 73019.
[+] Corresponding Author: E-mail dvsinghchauhan@gmail.com; dvsingh@ou.edu
Note: Submitted September 7, 2011; Revised November 22, 2011; Accepted November 23, 2011.

Table 1. Gradation of Mixes.

Material	Mix-1	Mix-2
1" Rock (%)	20	22
Manufactured Sand (%)	44	50
Sand (%)	11	13
RAP (%)	25	15
Sieve Size (mm)	Gradation (% Passing)	
25	100	100
19	98	98
12.5	87	87
9.5	80	80
4.75	58	62
2.36	37	40
1.18	25	27
0.6	19	20
0.3	12	12
0.15	4	5
0.075	2.9	2.8

RAP = Reclaimed Asphalt Pavement

Table 2. Volumetric Properties of Mixes.

Volumetric Properties	Mix-1	Mix-2
G_{mm}	2.505	2.523
G_{se}	2.671	2.677
G_{sb}	2.645	2.657
G_b	1.01	1.01
Binder Type	PG 64-22	PG 76-28
P_b (%)	4.1	4.1
Aggregate Type	Limestone	Limestone
Mix Type	Recycled	Recycled

G_{mm} = Maximum Theoretical Specific Gravity Mixture
G_{sb} = Bulk Specific Gravity of Aggregate
G_{se} = Effective Specific Gravity of Aggregate
G_b = Specific Gravity of Binder
P_b = Asphalt Content

The present study examines the effect of LTO-aging on two different HMA mixes containing different PG grade binders and RAP using the |*E**| test. The mechanistic empirical pavement design guide (MEPDG) recommends |*E**| as one of the fundamental properties of a mix in evaluating the long-term performance of a flexible pavement [21]. Previous studies show that |*E**| has a significant correlation with major pavement distresses, namely fatigue, rutting, and low temperature cracking [22-26]. This present study should be helpful in understanding the behavior of RAP-containing mixes.

Material

Two different types of plant produced HMA mixes were collected. The aggregates in Mix-1 have approximately 20% of 1" rock, 44% manufactured sand, 11% sand, 25% RAP, and 4.1% of unmodified PG64-22 binder. Similarly, the aggregates in Mix-2 contain approximately 22% of 1" rock, 50% manufactured sand, 13% sand, 15% RAP and 4.1% PG76-28 styrene-butadiene-styrene (SBS) modified binder. Both mixes contain a similar aggregate type (primarily limestone) and the same nominal maximum aggregate size (NMAS) of 19 mm. The RAP used for the production of these two mixes was taken from the same stockpile maintained at the selected plant site. The asphalt binders used in this study were obtained from the Valero Refinery in Ardmore, Oklahoma. These mixes are commonly used in Oklahoma for pavement construction. The gradations and other volumetric properties of Mix-1 and Mix-2 are given in Table 1 and Table 2, respectively.

Specimen Preparation

Since the loose mixes were collected from the production plant, no short-term aging was done in the laboratory. Therefore, to prepare the samples, the loose mixes were directly preheated in an oven at 150^{o}C for a duration of 1 to 2 hours. The compaction temperature of both the mixes was targeted in the range of 145^{o}C to 150^{o}C. Specimens were compacted using a Superpave Gyratory Compactor (SGC). The SGC machine was operated in height mode, which facilitates the machine to stop automatically when the desired height of sample is reached.

Initially, specimens of 150 mm in diameter and 167.5 mm in height with 6%, 8%, 10%, and 12±1% target air voids were prepared. A trial and error process was used to adjust the weight of the loose mix to obtain the desired target air voids in a compacted sample. Specimens compacted at 6% air voids (i.e., 94% of maximum density) represent a well-compacted pavement immediately after construction, while 8% to 10% air voids indicate an intermediate compaction (i.e., 90% to 92% of maximum density). Similarly, 12% air voids simulates lay-down density (i.e., 88% density) of a mix in the field. The selection of these four levels of air voids covers a practical range of compaction density encountered during the construction of a flexible pavement.

Three replicates of the specimens were compacted at each target level of air voids. The final test samples, 100 mm in diameter and 150 mm in height, were then cut and cored from the center of the SGC compacted samples. These specimens have the most consistent air void distribution in both vertical and radial directions [27]. Moreover, these are the specimen geometries currently recommended for the simple performance test [26] and used in the constitutive modeling of asphalt concrete in tension and compression [28-30]. These samples were used to conduct the dynamic modulus test. Volumetric analyses were conducted on the final compacted sample (100 mm in diameter and 150 mm in height) to obtain the effective binder content (V_{beff}), voids in mineral aggregates (VMA), voids filled with asphalt (VFA), and air voids (V_a) for both mixes. Table 3 summarizes the volumetric properties of the compacted specimens. Since samples have not undergone any LTO-aging in this stage, the compacted samples are referred to as un-aged samples.

Dynamic Modulus (|*E**|) Testing

|*E**| was measured for Mix-1 and Mix-2 for samples compacted at four different air voids of 6%, 8%, 10%, and 12%. |*E**| tests were conducted using a material testing service (MTS) servo-hydraulic

Table3. Volumetric Properties of Compacted Specimens.

		Mix-1 Specimen			Mix-2 Specimen		
Target Air Voids (%)	(%)	1	2	3	1	2	3
6	V_a	5.4	5.6	5.6	6.5	6.4	6.4
	VMA	14.1	14.3	14.3	14.9	14.8	14.7
	VFA	62.2	61.4	61.5	60.1	60.4	60.8
	V_{beff}	8.8	8.8	8.8	8.9	8.9	9.0
8	V_a	7.3	7.2	7.2	8.3	8.1	7.9
	VMA	15.8	15.7	15.7	16.5	16.3	16.1
	VFA	54.5	54.7	54.9	53.3	53.9	54.6
	V_{beff}	8.6	8.6	8.6	8.8	8.8	8.8
10	V_a	9.3	9.6	9.1	9.6	10.2	9.8
	VMA	17.7	17.9	17.5	17.7	18.3	17.9
	VFA	47.7	46.9	48.3	48.9	47.0	48.3
	V_{beff}	8.4	8.4	8.4	8.6	8.6	8.6
12	V_a	11.5	12.4	12.4	12.2	11.7	12.0
	VMA	19.7	20.4	20.4	20.0	19.6	19.9
	VFA	41.8	39.9	39.9	41.9	43.2	42.3
	V_{beff}	8.2	8.1	8.1	8.4	8.4	8.4

V_a = Air Voids; VMA = Voids in Mineral Aggregates
VFA = Voids Filled with Asphalt; V_{beff} = Effective asphalt content by volume

Table 4. Test Matrix for Dynamic Modulus.

Air Voids	Temperature	Frequency	Mix-1		Mix-2	
			Test Condition			
(%)	(°C)	(Hz)	Un-aged	Aged	Un-aged	Aged
6	4, 21, 40, 55	25, 10, 5, 1, 0.5, 0.1	✓	✓	✓	✓
8			✓	✓	✓	✓
10			✓	✓	✓	✓
12			✓	✓	✓	✓

testing system. Test specimen (100 mm in diameter and 150 mm in height) was placed in an environmental chamber and allowed to reach equilibrium (i.e., specified testing temperature of ±0.5°C). Specimen temperature was monitored using a dummy specimen with a thermocouple mounted at the center. Deformation of a specimen was measured using two linear variable differential transducers (LVDTs) mounted on a specimen at 100 mm gauge length. The accuracy in measuring the dynamic modulus with three specimens (two LVDTs on each specimen) is expected to range within ±15.0% [31].

Two friction-reducing end treatments, or teflon papers, were placed between the specimen ends and loading plates. To begin testing, a minimal contact load was applied to the specimen. A sinusoidal axial compressive load was applied to the specimen without impact in a cyclic manner. The test was conducted on each specimen at four different temperatures of 4°C, 21°C, 40°C, and 55°C, starting from the lowest temperature to the highest. For each temperature level, the test was conducted at different frequencies from the highest to the lowest (25 Hz, 10 Hz, 5 Hz, 1 Hz, 0.5 Hz, and 0.1 Hz).

Prior to testing, every specimen was conditioned by applying 200 cycles of load at a frequency of 25 Hz. The load magnitude was adjusted based on the material stiffness, air voids, temperature and frequency to keep the strain response within 50-150 micro-strains. The data was recorded for the last 5 cycles of each sequence. $|E^*|$ tests were performed according to AASHTO TP62-03 [31]. $|E^*|$ testing was done on both un-aged and LTO-aged specimens. A total of 288 $|E^*|$ (4 air voids x 4 temperatures x 6 frequencies x 3 specimens) values were measured in the laboratory for un-aged condition. The un-aged condition refers to the samples that did not go through the LTO-aging process. The measured $|E^*|$ on un-aged samples is referred to as un-aged $|E^*|$. Table 4 shows the test matrix used for conducting $|E^*|$ tests in the laboratory.

Long-Term Oven (LTO) Aging of Compacted Specimens

Since dynamic modulus testing is considered to be a non-destructive test, the same samples can be used for additional testing. Therefore, after completing dynamic modulus testing on un-aged samples, the samples continued on for LTO-aging. The samples compacted at four different air voids (i.e., 6%, 8%, 10%, and 12%) were LTO-aged in accordance with the AASHTO R30 method [32], which recommends aging the compacted specimens in a forced draft oven for 5 days at 85°C. This standard is expected to simulate the long-term aging of a mix in the field for over a period of 5 to 7 years, irrespective of environmental conditions and mix properties.

To avoid or minimize the slump during aging, specimens were wrapped in a wire mesh. Three steel clamps were used to hold the mesh in place. This method facilitated the highest amount of air circulation without allowing for any slump. Specimens were taken out of the oven after 5 days and allowed to cool at room temperature. $|E^*|$ measured under LTO-aged condition is referred to as aged $|E^*|$ in this paper.

Construction of Master Curves

$|E^*|$ of an HMA mix can be shifted along the frequency axis to form single characteristic master curves at a desired reference temperature or frequency [31]. Master curve is generated at a reference temperature of 21°C using the procedure outlined in Bonaquist et al. [33]. An approach developed by Bonaquist et al. [33] eliminates the lower temperature requirement. Therefore, the time required in conducting $|E^*|$ testing and master curve construction can be reduced. Eqs. (1) and (2) show the sigmoidal function and the shift factor used for fitting a master curve. The limiting maximum modulus (i.e., *Max* modulus) is estimated based on binder stiffness and mix volumetric data using Eqs. (3) and (4) [34]. A nonlinear optimization program, available in Microsoft Excel®, was used to simultaneously solve these unknown parameters. A total of 8 master curves were generated (4 un-aged and 4 LTO-aged conditions).

$$Log|E^*| = \delta + \frac{Max - \delta}{1 + \exp\left(\beta + \gamma\left[\log(f) + c\left(10^{(A + VTS\ \log(T_R))}\right) - \log\eta_{t=r}\right]\right)} \quad (1)$$

$$a(T) = \frac{f_r}{f} \quad (2)$$

$$|E^*|_m = P_c\left[4{,}200{,}000\left(1 - \frac{VMA}{100}\right) + 3|G^*|_b\left(\frac{(VMA)(VFA)}{10{,}000}\right)\right] + \frac{1 - P_c}{\left[\dfrac{\left(1 - \dfrac{VMA}{100}\right)}{4{,}200{,}000} + \dfrac{VMA}{3|G^*|_b(VFA)}\right]} \quad (3)$$

$$P_c = \frac{\left(20 + \dfrac{3|G^*|_b(VFA)}{VMA}\right)^{0.58}}{650 + \left(\dfrac{3|G^*|_b(VFA)}{VMA}\right)^{0.58}} \quad (4)$$

where *Max* is the maximum $|E^*|$ for a particular mix; f_r is the reduced frequency at reference temperature 21°C; f is the frequency at a particular temperature; $\eta_{t=r}$ is the binder viscosity at reference temperature 21°C; T_R is the temperature in Rankine; A is the regression intercept of viscosity-temperature curve; *VTS* is the regression slope of viscosity-temperature susceptibility; $a(T)$ is the shift factor as a function of temperature and age; and δ, β, γ, and c are the fitting parameters.

$|E^*|_m$ is the absolute value (maximum value) of asphalt mixture dynamic modulus (psi), $|G^*|_b$ is the absolute value of asphalt binder complex shear modulus (psi) (i.e., 145,000 psi), *VMA* is the voids in mineral aggregates in the compacted mixture (%), *VFA* is the voids filled with asphalt binder in the compacted mixture (%), and *Max* is the limiting maximum modulus of an asphalt mix.

The intercept (A) and slope (*VTS*) parameters pertaining to the temperature-viscosity graph of binder were taken from the MEPDG [21]. A and *VTS* were noted as 10.98 and -3.680 for PG64-22 binders and 9.2 and -3.024 for PG76-28 binders. The goodness-of-fit statistics, S_e/S_y (standard error of estimate and standard deviation), and correlation coefficient (R^2) reported in Pellinen and Witczak [24] were used to assess the validity of the correlation between laboratory measured modulus and master curve fit equation. Table 5 lists the statistical measurements and criteria used in the present study. The coefficients and fitting statistics of the master curves and shift factor curves for Mix-1 and Mix-2 are summarized in Table 6 and Table 7.

Table 5. Statistical Parameters Measured and the Criteria Used in the Study [24]

Rating	R^2	*Se/Sy*
Excellent	≥0.90	≤0.35
Good	0.70 - 0.89	0.36 - 0.55
Fair	0.40 - 0.69	0.56 - 0.75
Poor	0.20 - 0.39	0.76 - 0.90
Very Poor	≤0.19	≥0.90

Based on these criteria, the developed master curves (for un-aged and LTO-aged conditions) equations were found to be in excellent correlation with the laboratory measured data (S_e/S_y in the range of 0.04 to 0.15; R^2 approximating 0.99). Shift factors were calculated for un-aged and LTO-aged conditions at four different temperatures and four air voids. The developed master curves and shift factors are useful in the estimation of $|E^*|$ at a wide range of temperatures and frequencies for un-aged and aged conditions of an HMA mix.

Results and Discussion

Effect of Air Voids, Frequency and Temperature on |E*|

To show the effect of air voids on $|E^*|$, one particular frequency (10 Hz) and one temperature (21°C) were selected. For both mixes (Mix-1 and Mix-2), $|E^*|$ decreases with increasing air voids (Fig. 1). Similarly, Fig. 2 shows the variation of $|E^*|$ with test frequency at 6% air voids and 21°C test temperature. It can be seen from Fig. 2 that $|E^*|$ increased with increasing test frequencies.

Variation of $|E^*|$ with temperature at 6% air voids and 10 Hz loading frequency is shown in Fig. 3. Under a constant loading frequency, $|E^*|$ decreases with an increase in test temperature. The above trends of $|E^*|$ with temperature and frequency are consistent with the results reported by other researchers [35-37]. It is interesting to note that at all air voids, temperatures and frequencies Mix-1 (PG64-22 @25% RAP) resulted in higher $|E^*|$ compared to Mix-2 (PG76-28 @15% RAP). Thus, it is expected that the inclusion of a higher percentage of RAP results in a stiffer structure compared to a lower percentage of RAP. Similar results were observed for LTO-aged $|E^*|$.

Table 6. Master Curves and Shift Factor Parameters for Un-aged Condition.

Air Voids (%)	Max E^* (MPa)	δ	β	γ	c	R^2	S_e/S_y	Fit
			Mix-1					
6	23084	1.81	-1.02	-0.43	1.20	0.99	0.07	Excellent
8	22256	1.54	-0.98	-0.39	1.20	0.99	0.05	Excellent
10	21232	1.23	-0.86	-0.37	1.04	0.99	0.06	Excellent
12	19942	1.72	-0.41	-0.40	1.05	0.99	0.08	Excellent
			Mix-2					
6	22826	2.10	-0.25	-0.45	1.24	0.99	0.04	Excellent
8	22027	1.99	-0.24	-0.42	1.18	0.99	0.05	Excellent
10	21157	1.98	-0.17	-0.42	1.12	0.99	0.04	Excellent
12	20182	1.71	-0.12	-0.37	1.13	0.99	0.05	Excellent

Air Voids (%)	Shift Factors log(aT) Mix-1 4° C	Mix-1 21° C	Mix-1 40° C	Mix-1 55° C	Mix-2 4° C	Mix-2 21° C	Mix-2 40° C	Mix-2 55° C
6	2.66	0.00	-2.23	-3.60	2.24	0.00	-1.96	-3.20
8	2.65	0.00	-2.22	-3.58	2.13	0.00	-1.86	-3.04
10	2.30	0.00	-1.93	-3.11	2.02	0.00	-1.77	-2.89
12	2.32	0.00	-1.95	-3.14	2.04	0.00	-1.78	-2.91

Table 7. Master Curves and Shift Factor Parameters for Aged Condition.

Air Voids (%)	Max E^* (MPa)	δ	β	γ	c	R^2	S_e/S_y	Fit
			Mix-1					
6	23084	2.41	-0.86	-0.53	1.05	0.97	0.13	Excellent
8	22256	1.44	-1.40	-0.33	1.42	0.98	0.15	Excellent
10	21232	1.70	-0.93	-0.40	1.09	1.00	0.07	Excellent
12	19942	2.21	-0.42	-0.53	1.01	0.99	0.07	Excellent
			Mix-2					
6	22837	2.33	-0.52	-0.50	1.28	0.99	0.05	Excellent
8	22044	2.09	-0.54	-0.42	1.19	1.00	0.04	Excellent
10	21179	1.65	-0.66	-0.36	1.23	0.99	0.10	Excellent
12	20210	1.99	-0.28	-0.38	1.23	1.00	0.11	Excellent

Air Voids (%)	Shift Factors log(aT) Mix-1 4° C	Mix-1 21° C	Mix-1 40° C	Mix-1 55° C	Mix-2 4° C	Mix-2 21° C	Mix-2 40° C	Mix-2 55° C
6	2.33	0.00	-1.96	-3.15	2.32	0.00	-2.03	-3.31
8	3.15	0.00	-2.65	-4.26	2.16	0.00	-1.88	-3.08
10	2.41	0.00	-2.03	-3.26	2.22	0.00	-1.94	-3.17
12	2.24	0.00	-1.89	-3.04	2.22	0.00	-1.94	-3.17

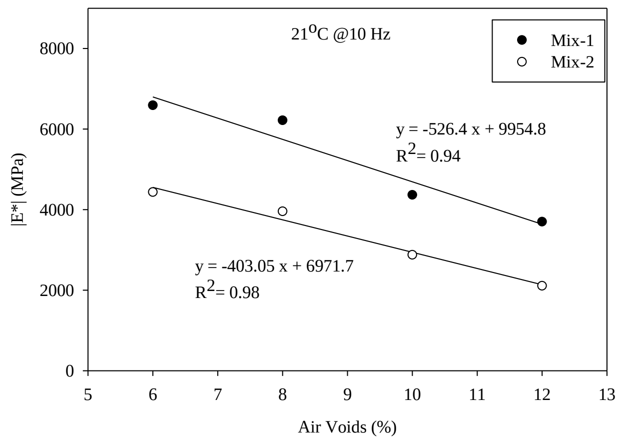

Fig. 1. Variation of |E^*| with Air Voids.

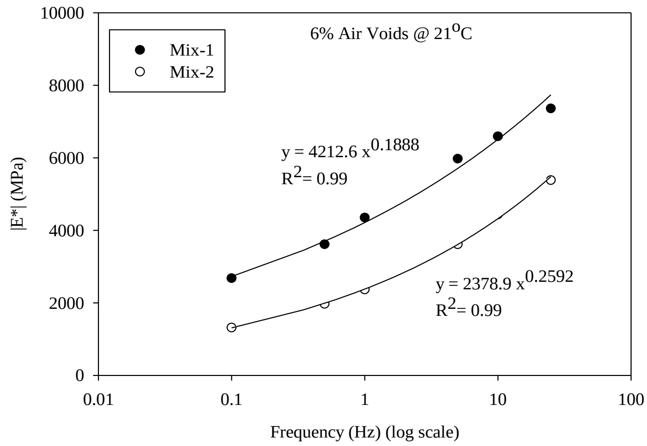

Fig. 2. Variation of |E^*| with Frequency.

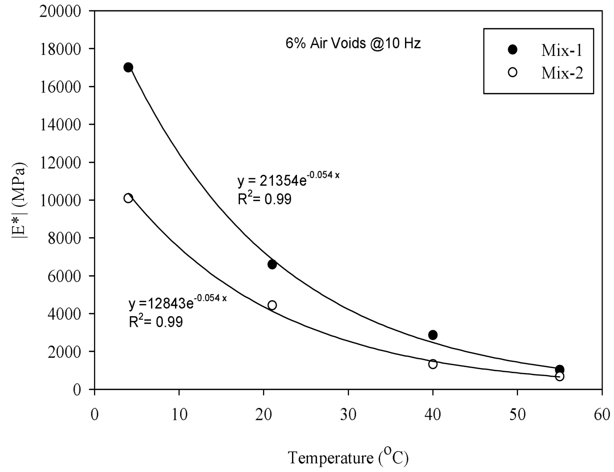

Fig. 3. Variation of $|E^*|$ with Temperature.

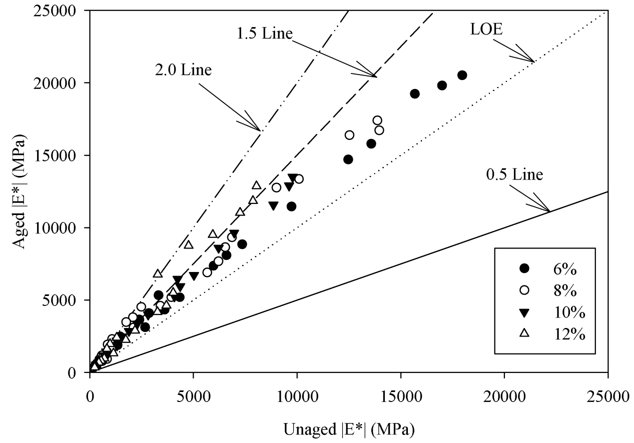

Fig. 4. Effect of LTO-Aging on Mix-1.

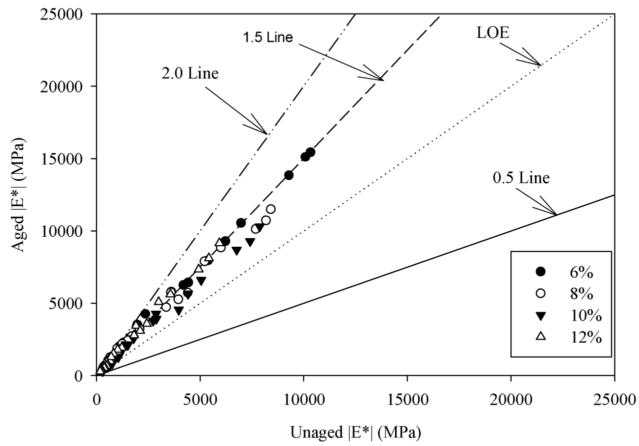

Fig. 5. Effect of LTO-Aging on Mix-2.

Effect of Long-Term Oven (LTO) Aging on $|E^*|$

Effects of LTO-aging on $|E^*|$, for Mix-1 and Mix-2, are evaluated by plotting un-aged and aged $|E^*|$ on the line of equality (LOE) plot. The LOE plot was divided into different regions by drawing lines at

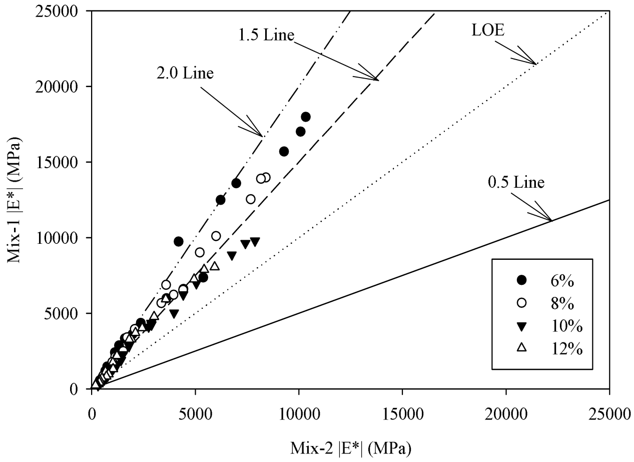

Fig. 6. Comparison of $|E^*|$ for Mix-1 and Mix-2 for Un-aged Condition.

different slopes. For example, the LOE line is drawn at 45° slope, where the ratio of aged and un-aged $|E^*|$ is equal to 1. Similar lines were drawn into the LOE plot at 0.5, 1.5, and 2 ratios. These lines are called the 0.5 line, 1.5 line, and 2 line, respectively. If a point falls on the 0.5 line, it indicates that aged $|E^*|$ is 50% less than un-aged $|E^*|$. Similarly, if a point falls on the 1.5 and 2 lines, it indicates that the aged $|E^*|$ is 50% and 100% higher than the un-aged $|E^*|$. Fig. 4 shows the different regions marked on the LOE plot.

Fig. 4 shows a comparison of un-aged and aged $|E^*|$ for Mix-1. It was found that LTO-aging causes a significant impact on $|E^*|$ at all air void levels. Aged $|E^*|$ falls between the 2.0 line and the LOE line, indicating that aging increases $|E^*|$ by a factor greater than 1 (Fig. 4). The process of oxidation in binders (aging) form polar compounds that tend to increase the amount of asphaltenes. These asphaltenes contribute to a solid structure of asphalt binder that leads to increased binder stiffness and viscosity [38-39]. Average percentage change in $|E^*|$ due to LTO-aging for 6%, 8%, 10%, and 12% air voids was observed at approximately 42%, 53%, 50%, and 60%, respectively. Thus, specimens with a higher percentage of air voids aged more when compared to specimens with lower air voids. It is believed that specimens with higher air voids have an open structure of aggregates that allows free circulation of air inside the specimen. This causes more hardening of the binder, whereas a structure with lower air voids narrow down the free circulation of air inside the specimen, resulting in relatively less aging of the binder.

Similar observations were made for Mix-2, where the change in $|E^*|$ was observed in the range of 60% to 64% (Fig. 5). It is interesting to note that LTO-aging causes more impact on Mix-2 as compared to Mix-1. For example, an increase in $|E^*|$ due to LTO-aging varied from 40% to 60% for Mix-1 and from 60% to 64% for Mix-2. This may be due to the fact that Mix-1 contains a higher percentage of RAP (25%) compared to Mix-2 (15%). It is expected that the higher percentage of RAP causes Mix-1 to age slowly.

Kiggundu et al. [40] show that mixes prepared from the recycled binder generally age at a slower rate than virgin mixes. It is believed that RAP binder has already undergone oxidation, which tends to

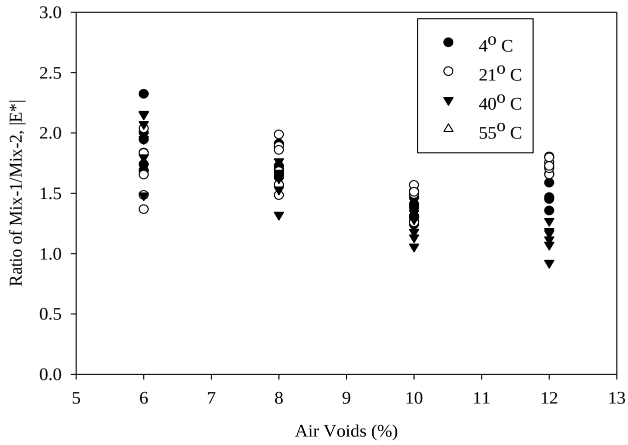

Fig. 7. Spread of Ratio of |*E**| for Mix-1 and Mix-2 for Un-aged Condition.

retard the rate of hardening [11, 40]. Moreover, the mixing of a higher percentage of RAP with virgin binder causes significant changes in the chemical and rheological properties of the binder, forming a complex structure. Aging is a very complex process that is influenced by many factors, such as temperature, moisture, traffic, ultra-violet ray, air void distribution and thickness of pavement layers. The results in the present study are consistent with the previous study done by Daniel et al. [19] and Francken et al. [20].

Comparison of Mix-1 and Mix-2

Un-aged Condition

The performance of Mix-1 and Mix-2 was compared for both un-aged and LTO-aged conditions. A comparison of two mixes was done by using two different approaches: plotting the |*E**| of Mix-1 and Mix-2 on the LOE plot and comparing the master curve constructed at reference temperature 21°C.

Fig. 6 shows the measured |*E**| for Mix-1 and Mix-2 for different air voids and temperatures. The measured |*E**| for Mix-1 falls above the LOE, indicating that Mix-1 results in higher |*E**| compared to Mix-2. At high temperature, Mix-1 and Mix-2 resulted in an approximately equal |*E**|. This indicates that, at high temperature, the effect of binder is not significant. However, since Mix-1 contains higher amounts of RAP (25%) than Mix-2 (15%), Mix-1 should still result in a higher |*E**| at higher temperature. To understand this further, the ratio of |*E**| for Mix-1 and Mix-2 (Mix-1/Mix-2) with air voids were plotted at four different temperatures (Fig. 7). At all temperatures, Mix-1 resulted in a higher |*E**| compared to Mix-2. The average |*E**| ratio ranged from 1.2 to 1.7, depending on the air voids and temperatures.

As noted earlier, a virgin mix (without any RAP) with a stiffer grade binder (i.e., PG76-28) would result in a higher modulus compared to a mix with a lower grade binder (i.e., PG64-22). However, analyses of results show that this behavior is not true if the mix contains RAP. The binder in a RAP has already undergone aging in the field, causing a change in its chemical composition. Mixing RAP binder with unmodified or modified binders forms a more complex structure that is not easily understood. Thus, the inclusion of RAP binder has a significant impact on the stiffness of an HMA mix.

For example, in the present study, Mix-1 with unmodified PG64-22 binder and 25% of RAP resulted in higher |*E**| compared to Mix-2 with SBS modified PG76-28 binder and 15% RAP. The higher modulus at high temperature is beneficial in controlling rutting. However, it is not considered as good at lower temperature, since it may result in low temperature cracking. Therefore, it is important to examine such behavior of RAP-containing HMA mixes to predict the performance of flexible pavements.

A comparison of Mix-1 and Mix-2 was further made by comparing the master curves constructed at reference temperature 21°C for all four air voids. Fig. 8 shows the master curves for both mixes. A comparison of Mix-1 and Mix-2 using the master curve is an important technique, as it allows the comparison of |*E**| at a wide range of temperatures and frequencies. In general, Mix-1 (25% of RAP) produces higher |*E**| compared to Mix-2 (15% of RAP) at all combinations of temperature and frequency, expect at high temperature (low frequency). At a high temperature, the binder starts flowing, and it does not hold aggregate particles together. Therefore, the aggregate's morphology, namely its angularity and texture, plays an important role [35].

Aged Condition

A comparison of LTO-aged |*E**| of Mix-1 and Mix-2 was made by plotting them on the LOE graph and generating master curves at 21°C. Fig. 9 shows the LOE plots for both mixes. At all temperatures, Mix-1 shows a higher |*E**| compared to Mix-2. The average modulus ratio ranged from 1.4 to 1.5, depending on air voids and temperatures (Fig. 10). The difference in |*E**| for Mix-1 and Mix-2 decreased after LTO-aging. For example, in un-aged conditions, the highest ratio of |*E**| for Mix-1 and Mix-2 was observed at 1.7, while this ratio was calculated at approximately 1.5 in LTO-aged condition.

A comparison of master curves of LTO-aged |*E**| is presented in Fig. 11. Mix-1 resulted in a higher |*E**| compared to Mix-2 for all combinations of temperature and frequency. In aged condition, master curves for both mixes seem closer at particular air voids, indicating a lesser difference between the two mixes. The master curves depict that the modulus reaches an equilibrium stage at low and higher temperatures.

Statistical Analysis

The performance of Mix-1 and Mix-2 was further compared through a statistical analysis, called pair-wise student t-test, at the significance level of 0.05. The null hypothesis for this analysis was that the difference in mean |*E**| for Mix-1 and Mix-2 is equal to zero ($H_0 = \mu_{Mix\text{-}1} = \mu_{Mix\text{-}2}$). Statistically, a significant factor p-value of less than 0.05 indicates that the null hypothesis was rejected, and the means of the data sets are not statistically equal. Comparisons were made for both un-aged and LTO-aged conditions at four different air voids, four temperatures, and a frequency of 10 Hz. Table 8 shows the results of the statistical analyses.

At low air voids (6%), statistical analyses show that Mix-1

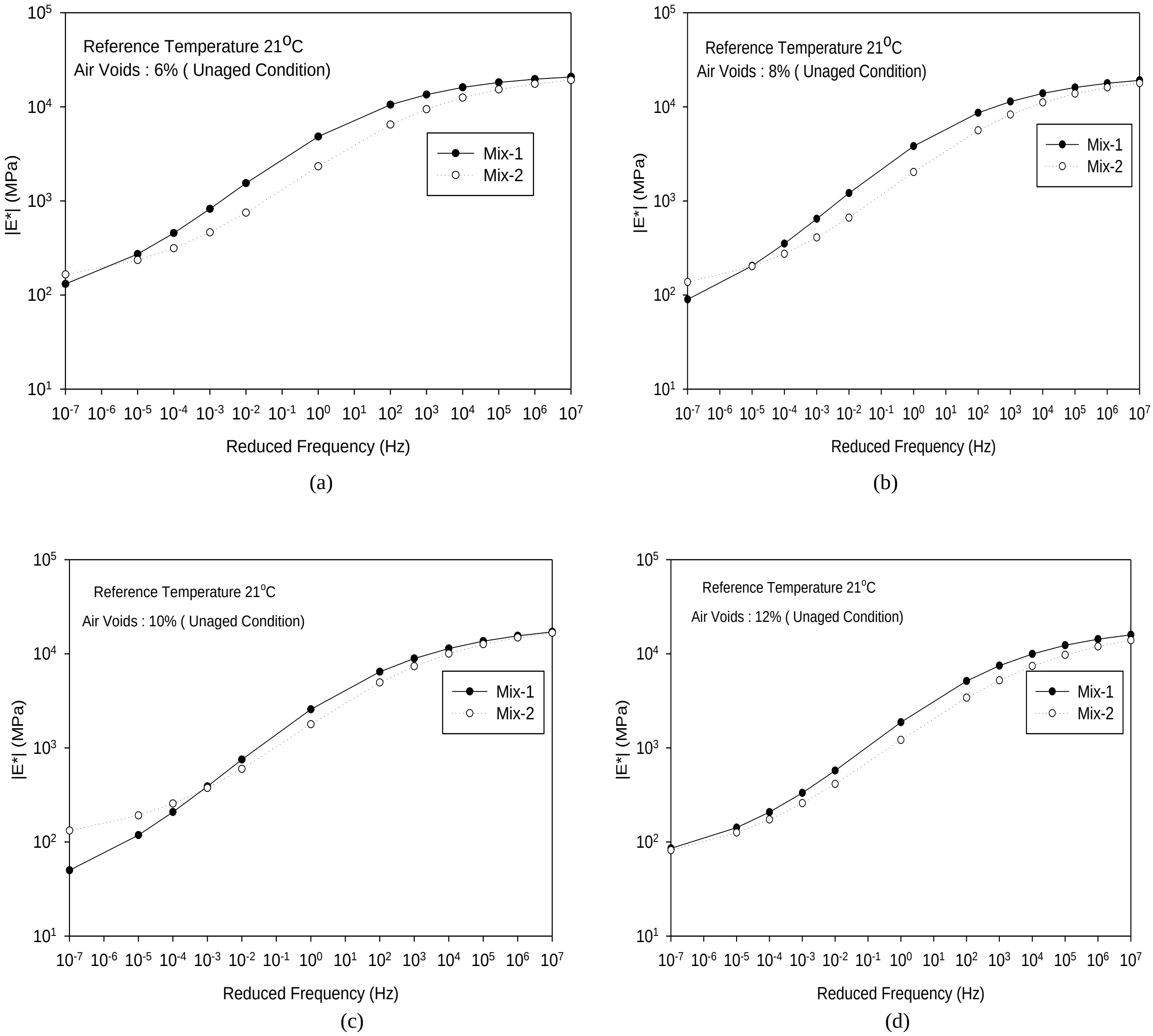

Fig. 8. Master Curves for Un-aged Condition at Four Air Voids: (a) 6% (b) 8% (c) 10% (d) 12%.

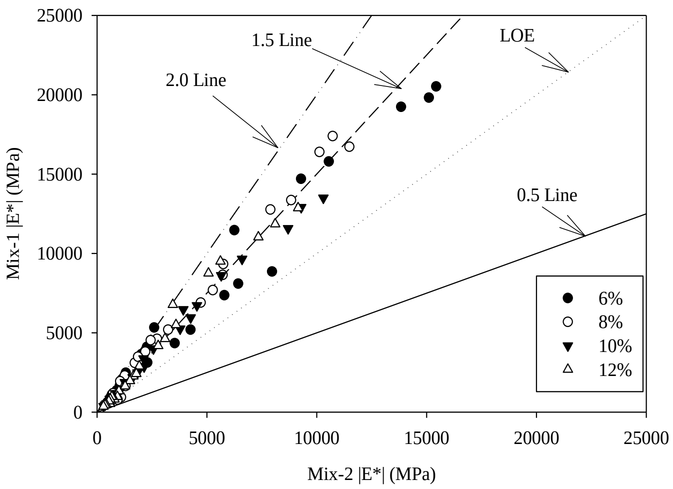

Fig. 9. Comparison of |*E**| for Mix-1 and Mix-2 for LTO-Aged Condition.

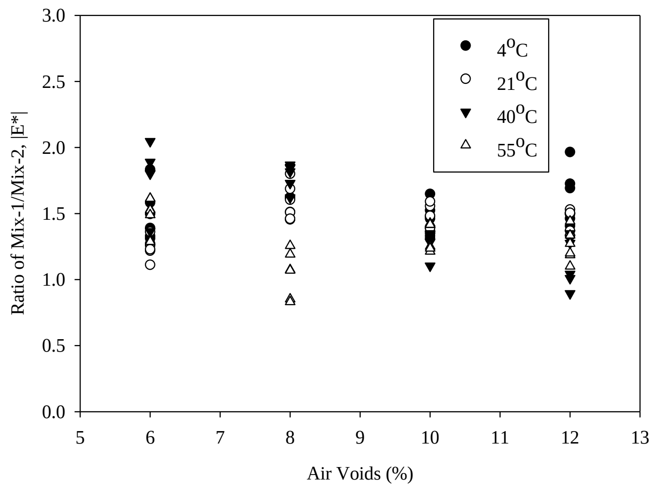

Fig. 10. Spread of the Ratio of |*E**| in Mix-1 and Mix-2 for LTO-Aged Condition.

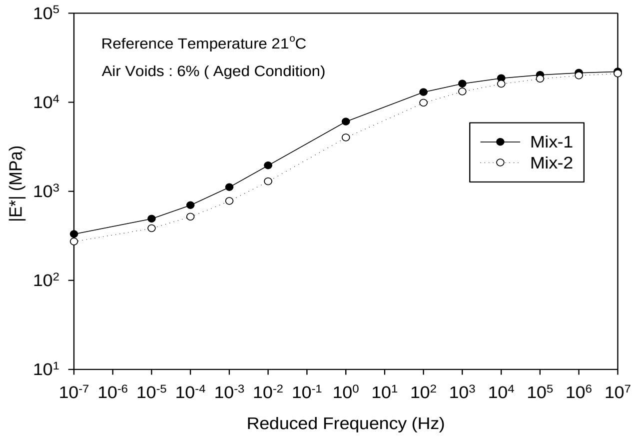

(a)

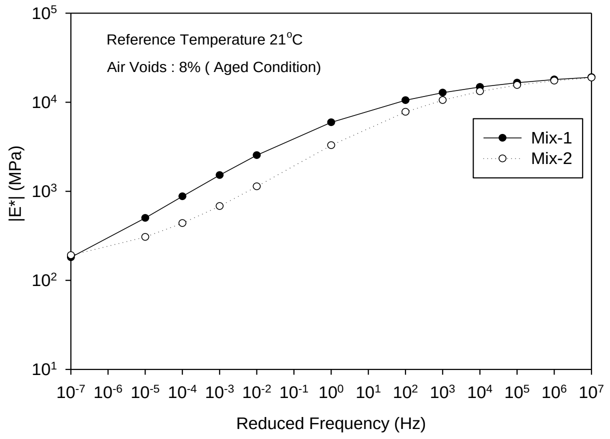

(b)

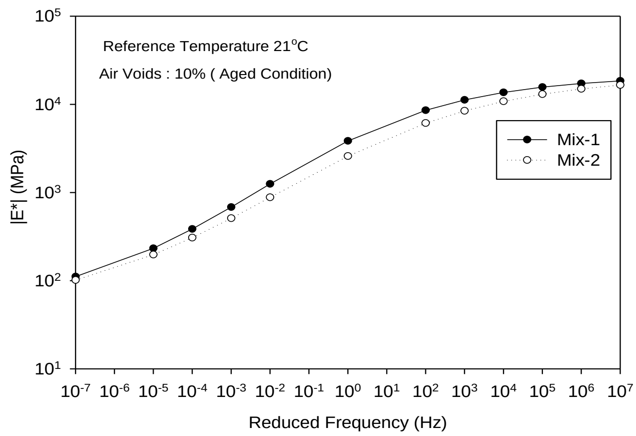

(b)

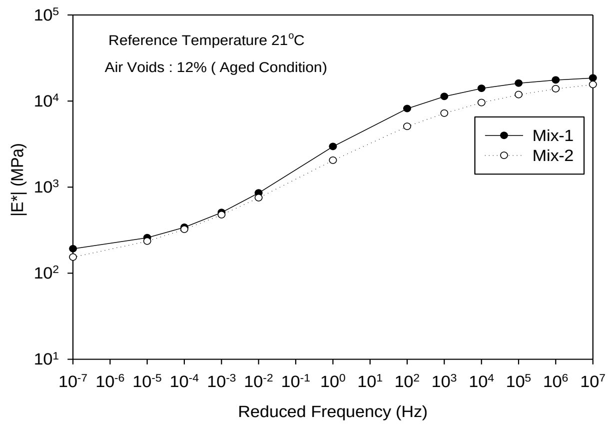

(d)

Fig. 11. Master Curves for LTO-aged Condition at Four Air Voids: (a) 6% (b) 8% (c) 10% (d) 12%.

Table 8. Statistical Analyses of Un-aged and Aged Dynamic Modulus.

Un-aged at 10 Hz Frequency								
Temperature (°C)	Air Voids (%)							
	6		8		10		12	
	p value	Sig.	p value	Sig.	p value	Sig.	p value	Sig.
4	0	Y	0.015	Y	0	Y	0.020	Y
21	0.018	Y	0.018	Y	0.029	Y	0.030	Y
40	0	Y	0	Y	0.055	N	0.200	N
55	0.033	Y	0.200	N	0.410	N	0.080	N
Aged at 10 Hz Frequency								
Temperature (°C)	Air Voids (%)							
	6		8		10		12	
	p value	Sig.	p value	Sig.	p value	Sig.	p value	Sig.
4	0.13	N	0.033	Y	0.096	N	0.032	Y
21	0.03	Y	0.011	Y	0.027	Y	0.031	Y
40	0	Y	0.015	Y	0.07	N	0.038	Y
55	0	Y	0.39	N	0.08	N	0.28	N

(PG 64-22 at 25% RAP) results in a higher |*E**| compared to Mix-2 (PG 76-28 at 15%RAP) for all temperatures. For both un-aged and LTO-aged conditions, no statistically significant differences exist between Mix-1 and Mix-2 at higher air voids (8% to 12%) and higher temperature (55°C).

This indicates that, at a higher temperature, binder does not influence |*E**|. Overall, the statistical analyses reveal that a higher percentage of RAP causes a higher magnitude of |*E**| compared to a mix with a lower percentage of RAP.

Concluding Remarks

The present study was undertaken to evaluate the performance of two different HMA mixes containing RAP. The following conclusions can be drawn from the results and discussions presented:

1. The degree of compaction (amount of air voids), temperature and frequency have a significant impact on $|E^*|$. A proper selection of these parameters is important in predicting the response of a flexible pavement.
2. LTO-aging resulted in an increase, approximately 42% to 60%, in $|E^*|$, depending on the amount of RAP and air voids. Specimens having higher air voids aged more rapidly compared to specimens with lower air voids.
3. Mixes with higher percentages of RAP aged more slowly compared to mixes with a lower percentage of RAP.
4. The higher the quantity of RAP, the stiffer the HMA mix, irrespective of binder grade.

The present study should be helpful in the selection of RAP in HMA mix designs and pavement construction. It is recommended that similar studies be conducted for mixes produced with other grades of unmodified and polymer modified binders and with different amounts of RAP. Furthermore, it is recommended that additional studies be conducted to evaluate the effects that different percentages of RAP have on the grade of asphalt binder.

Acknowledgments

The authors gratefully acknowledge the support of Volvo Construction Equipment Company in Shippensburg, PA, the Oklahoma Transportation Center in Oklahoma City, OK, and Haskell Lemon Construction Company in Oklahoma City, OK during the course of this research. The authors are also thankful to Imran Asif and Beainy Fares for their help in collecting the mixes from the plant.

References

1. Al-Qadi, I.L., Elseifi, M.A., and Carpenter, S.H. (2007). Reclaimed Asphalt Pavement- A Literature Review, *Report No. FHWA-ICT-07-001*, Illinois Center for Transportation (ICT), Urbana, IL.
2. McDaniel, R. and Anderson, R.M. (2001). Recommended Use of Reclaimed Asphalt Pavement in the Superpave Mix Design Method: Technician's Manual, *NCHRP Report No. 452*, Washington, DC, USA.
3. Federal Highways Administration (2010). Recycled Materials in Roadway Construction: The Many Ways of Going Green, http://www.fhwa.dot.gov/publications/focus/10apr/01.cfm (last accessed: April 30, 2012).
4. Kennedy, T.W., Tam, W.O., and Solaimanian, M. (1998). Optimizing Use of Reclaimed Asphalt Pavement with the SuperPave System, *Journal of the Association of Asphalt Paving Technologists*, Vol. 67, pp. 311-333.
5. Page, G.C. and Murphy, K.H. (1987). Hot-Mix Recycling Saves Florida DOT $38 Million, *Asphalt*, Vol. 1, No.1.
6. Huang, B., Zhang, Z., and Kinger, W. (2004). Fatigue Crack Characteristics of HMA Mixtures Containing RAP, *Proceedings of the 5th International RILEM Conference on Cracking in Pavements*, Limoges, France, pp. 631-638.
7. Li, X., Clyne, T.R., and Marasteanu, M.O. (2004). Recycled Asphalt Pavement (RAP) Effects on Binder and Mixture Quality, *Report No. MN/RC – 2005-02*, Minnesota Department of Transportation, St. Paul, MN, USA.
8. Little, D.H. and Epps, J.A. (1980). Evaluation of Certain Structural Characteristics of Recycled Pavement Materials, *Journal of the Association of Asphalt Paving Technologists*, Vol. 49, pp. 219-251.
9. Little, D.H., Holmgreen, R.J., and Epps, J.A. (1981). Effect of Recycling Agents on the Structural Performance of Recycled Asphalt Concrete Materials, *Journal of the Association of Asphalt Paving Technologists*, Vol. 50, pp. 32-63.
10. Brown, E.R. (1984). Evaluation of Properties of Recycled Asphalt Concrete Hot Mix. U.S. Army Engineer Waterways Experiment Station, *Final Report # CL-84-2*.
11. Meyers, F., Tessier, G.R., Haas, R., and Kennedy, T.W. (1983). Study of Hot Mix Recycling of Asphalt Pavements. Roads and Transportation Association of Canada, *Report # TP 2964 E*, Ottawa, Ontario.
12. Kandhal, P.S., Brown, E.R., and Cross, S. (1989). Guidelines for Hot Mix Recycling in Georgia, *Final Report, Project No. 8807*, Auburn Univ., Auburn, AL, USA.
13. Li, X., Marasteanu, M.O., Christopher W., and Clyne, T.R. (2008). Effect of RAP (Proportion and Type) and Binder Grade on the Properties of Asphalt Mixtures, *Transportation Research Board 86th Annual Meeting*, Washington, DC, USA.
14. McDaniel, R.S., Slah, A., Huber, G.A., and Gallivan, V. (2007). Investigation of Properties of Plant-Produced RAP Mixtures, *Transportation Research Board 86th Annual Meeting*, Washington, DC, USA.
15. Kandhal, P.S. and Mallick, R.B. (1997). Pavement Recycling Guidelines for State and Local Governments – Participant's Reference Book, *Report No. FHWA-SA-98-042*, National Center for Asphalt Technology, Auburn, AL, USA.
16. McDaniel, R.S., Soleymani, H., Anderson, R.M., Turner, P., and Peterson, R. (2000). Incorporation of Reclaimed Asphalt Pavement in the Superpave System, *NCHRP 9-12*, National Cooperative Highway Research Program, Transportation Research Board.
17. McDaniel, R.S., Soleymani, H., and Slah, A. (2002). Use of Reclaimed Asphalt (RAP) under Superpave Specifications, Report No. *FHWA/IN/JTRP-2002/6*, North Central Superpave Center, West Lafayette, IN, USA.
18. Xiao, F., Amirkhanian, S., and Juang, C.H.M. (2007). Rutting Resistance of Rubberized Asphalt Concrete Pavements Containing Reclaimed Asphalt Pavement Mixtures, *Journal of Materials in Civil Engineering*, 19(6), pp.475-483.
19. Daniel, J.S., Kim, Y.R., and Lee, H.J. (1998). Effects of Aging on Viscoelastic Properties of Asphalt-Aggregate Mixtures, *Transportation Research Record*, No. 1630, pp. 21-27.

20. Francken, L., Vanelstraete, A., and Verhasselt, A. (1997). Long Term Ageing of Pure and Modified Bitumen: Influence on the Rheological Properties and Relation with the Mechanical Performance of Asphalt Mixtures, *8th International Conference on Asphalt Pavements*, Vol. 2, pp. 1259-1278.
21. Mechanistic Empirical Pavement Design Guide (MEPDG) (2004). Development of the 2002 Guide for the Design of New and Rehabilitated Pavement Structured: Phase II, Transportation Research Board, Washington, DC, USA.
22. Goh, S.W., You, Z., Williams, R.C., and Li, X. (2011). Preliminary Dynamic Modulus Criteria of HMA for Field Rutting of Asphalt Pavements: Michigan's Experience, *Journal of Transportation Engineering*, 137(1), pp.37-45.
23. Loulizi, A., Flintsch, G., Al-Qadi, I., and Mokarem, D. (2006). Comparing Resilient Modulus and Dynamic Modulus of Hot Mix Asphalt as Material Properties for Flexible Pavement Design, *Transportation Research Record*, No. 1970, pp. 161-170.
24. Pellinen, T.K. and Witczak, M.W. (2002). Use of Stiffness of Hot-Mix Asphalt as a Simple Performance Test, *Transportation Research Record*, No. 1789, pp. 80-90.
25. Shenoy, A. and Romero, P. (2002). Standardized Procedure for Analysis of Dynamic Modulus (E*) Data to Predict Asphalt Pavement Distresses, *Transportation Research Record*, No. 1789, pp. 173-182.
26. Witczak, M.W., Kaloush, K., Pellinen, T., El-Basyouny, M., and Von-Quintus, H. (2002). Simple Performance Test for Superpave Mix Design, *NCHRP Report 465*, National Research Council, Washington, DC, USA.
27. Chehab, G., O'Quinn, R.E., and Kim, Y.R. (2000). Specimen Geometry Study for Direct Tension Test Based on Mechanical Tests and Air Void Variation in Asphalt Concrete Specimens Compacted by Superpave Gyratory Compactor, *Transportation Research Record*, No. 1723, pp. 125–132.
28. Schwartz, C.W., Gibson, N., and Schapery, R.A. (2002). Time–Temperature Superposition for Asphalt Concrete at Large Compressive Strains, *Transportation Research Record*, No. 1789, pp. 101-112.
29. Chehab, G. R. (2002). Characterization of Asphalt Concrete in Tension Using a Visco-Elasto-Plastic Model, *PhD Dissertation*, North Carolina State University, Raleigh, NC, USA.
30. Daniel, J. S. (2001). Development of a Simplified Fatigue Test and Analysis Procedure Using a Viscoelastic, Continuum Damage Model and Its Implementation to WesTrack Mixtures, *PhD Dissertation*, North Carolina State University, Raleigh, NC, USA.
31. American Association of State Highway and Transportation Officials (AASHTO) (2006). Standard Method of Test for Determining Dynamic Modulus of Hot-Mix Asphalt Concrete Mixtures: TP62-03, *AASHTO Provisional Standards*, Washington, DC, USA.
32. American Association of State Highway and Transportation Officials (AASHTO) (2002). Standard Practice for Mixture Conditioning of Hot Mix Asphalt (HMA): *AASHTO R30*, Washington, DC, USA.
33. Bonaquist, R. and Christensen, D.W. (2005). Practical Procedure for Developing Dynamic Modulus Master Curves for Pavement Structural Design, *Transportation Research Record*, No. 1929, pp. 208-217.
34. Christensen, D.W., Pellinen, T., and Bonaquist, R.F. (2003). Hirsch Model for Estimating the Modulus of Asphalt Concrete, *Journal of the Association of Asphalt Paving Technologists*, Vol. 72, pp. 97–121.
35. Huang, B., Shu, X., and Bass, J. (2008). Investigation of Simple Performance Characteristics of Plant-Produced Asphalt Mixtures in Tennessee, *Transportation Research Record*, No. 2057, pp. 140-148.
36. Bayat, A. and Knight, M. (2010). Investigation of Hot-Mix Asphalt Dynamic Modulus Using Field Measured Pavement Response, *89th Annual Meeting of Transportation Research Board*, Washington, DC, USA, CD-ROM.
37. You, Z., Adhikari, S., and Dai, Q. (2008). Three Dimensional Discrete Element Models for Asphalt Mixtures, *Journal of Engineering Mechanics*, 134(12), pp. 1053-1063.
38. Liu, M., Ferry, M.A., Davison, R.R., Glover, C.J., and Bullin, J.A. (1998). Oxygen Uptake as Correlated to Carbonyl Growth in Aged Asphalts and Asphalt Corbett Fractions, *Industrial and Engineering Chemistry Research*, 37(12), pp. 4669-4674.
39. Liu, M.M., Lin, M.S., Chaffin, J.M., Davison, R.R., Glover, C.J., and Bullin, J.A. (1998). Oxidation Kinetics of Asphalt Corbett Fractions and Compositional Dependence of Asphalt Oxidation, *Petroleum Science and Technology*, 16(7-8), p.827.
40. Kiggundu, B.M., Humphrey, B.N., and Zallen, D.M. (1985). Recycling Agent Selection and Tentative Specification, *Final Report #ESL-TR-84-47*, New Mexico Engineering Research Institute.